Quantum governor: Automatic quantum control and reduction of the influence of noise without measuring

S. Kallush and R. Kosloff
The Fritz Haber Research Center, The Hebrew University of Jerusalem, Jerusalem 91904, Israel
(Received 2 November 2005; published 17 March 2006)

The problem of automatically protecting a quantum system against noise in a closed circuit is analyzed. A general scheme is developed built from two steps. First, a distillation step is induced in which undesired components are removed to another degree of freedom of the system. Later a recovering step is employed in which the system gains back its initial density. An optimal-control method is used to generate the distilling operator. The scheme is demonstrated by a simulation of a two-level bit influenced by white noise. Undesired deviations from the target were shown to be reduced by at least two orders of magnitude on average. The relations between the quantum version of the classical Watt's governor and the field of quantum information are also discussed.

DOI: 10.1103/PhysRevA.73.032324 PACS number(s): 03.67.Pp, 32.80.Qk

I. INTRODUCTION

Watt's governor (WG), which was built in 1782, might be the very first machinery to solve automatically a control problem. As an automatic control tool, Watt's governor aims to conserve some physical properties of a system subject to stochastic noise while maintaining its internal dynamics. Schematically, the WG can be viewed as a two-step process, measurement and correction. At the first step a measurement of the system is performed to check whether the constraint has been violated. Next, if such a violation was found, a correction step takes place, and drives the system back to the allowed boundaries.

A quantum governor is a natural requirement when the limit of nanomachines is approached. Quantum computing [1–4] is another candidate for such a device. However, quantum mechanics imposes nontrivial restrictions on the development of the quantum governor (QG). A measurement, which is a main feature of the classical WG, intervenes in the dynamics of quantum systems and it therefore should be avoided or reduced to a minimum.

A control scheme is traditionally categorized as either an open-loop or a closed-loop control [5,6]. In the closed-loop control scheme one tries to extract information by feedback from the quantum system in a way that allows control of the system [7,8]. Within this scheme, a controlled collapse of some of the wave function occurs and converts some of the quantum variables of the system into classical parameters. One needs therefore to delicately balance the amount of withdrawn information in order to conserve the quantum character of the system. Feedback control of quantum systems has being extensively studied during recent years by several groups [7–10].

An open-loop control scheme corrects the system without any measurement. In order to realize the QG a tool that distills quantum systems in some automatic fashion has to be built. Distillation steps usually reduce the density of the system, and hence, in order to conserve the density of a controlled system, an extra step to enrich the system and compensate for the losses is also required.

In this paper we suggest and demonstrate a physical realization for an open-loop QG scheme. Our open-loop QG is a two-step routine (cf. Fig. 1). The scheme starts from an initial state, for example a diatomic molecule in its ground electronic and vibrational state. This state is then disturbed by noise. At the first stage of action, an external field is applied to the system with the purpose of distilling the undesired components. The rejected components are moved to another degree of freedom of the system, in the present model to an excited electronic state. At the next stage, the freely evolving dynamics are set to enrich the initial state and return it back to the initial density.

We will show that the distillation step can be performed by a particular unitary transformation. Recently, optimal-control theory (OCT) has been applied to find the field generating the unitary operation [11–13]. In the present paper the methods of Refs. [11,12] are generalized to obtain the control field for nonunitary operations under nonunitary time evolution governed by the Liouville equation for open quantum systems. This control field is then employed to derive the distillation stage of the QG. This step is followed by a field-free propagation of the system leading to the desired reconstructed state.

In this paper the QG model is presented along with the tools required for its construction. In Sec. II a simple QG model is presented. Section III elaborates on the OCT mathematical considerations required to achieve the distilling transformation. Section IV presents simulations of the QG. A discussion and conclusion are presented in Sec. V.

II. THE QG MODEL

The Hamiltonian of the quantum governor model is partitioned to

$$\hat{\mathbf{H}} = \hat{\mathbf{H}}^0 + \hat{\mathbf{H}}_{noise} + \hat{\mathbf{H}}_G \tag{1}$$

where $\hat{\mathbf{H}}^0$ is the free Hamiltonian of the system, $\hat{\mathbf{H}}_{noise}$ is the stochastic noise, and $\hat{\mathbf{H}}_G$ is the control part, governed by an external field. The automatic control scheme could be ap-

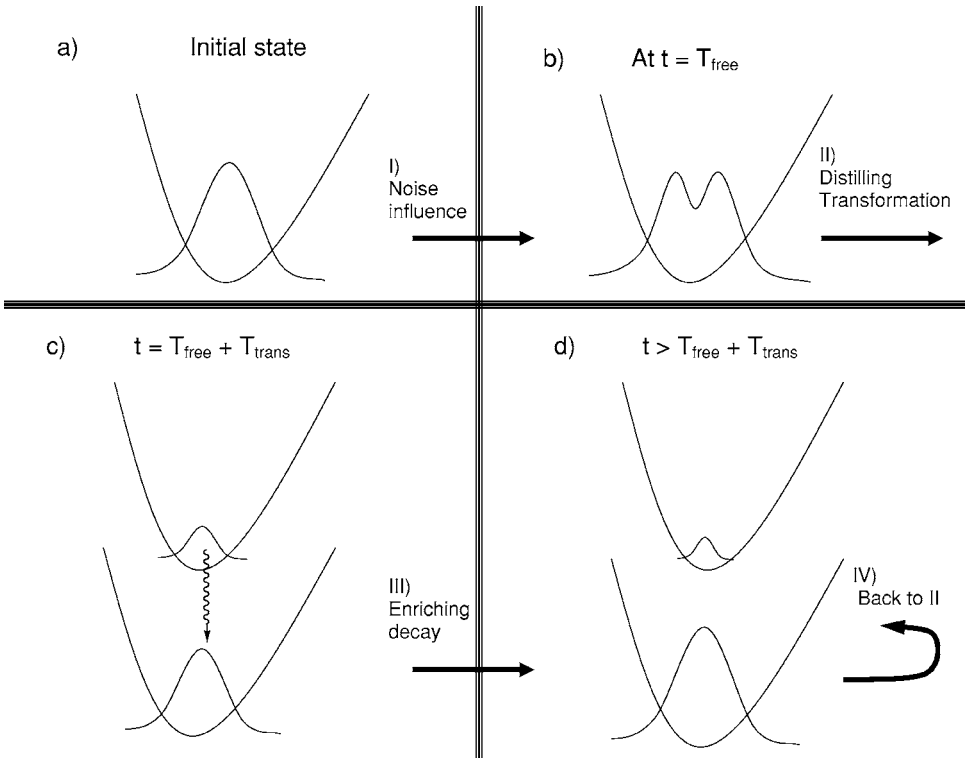

FIG. 1. Schematic principles of the QG. (a) An initial state is propagated under the influence of noise. (b) The initial state after the distortion. (c) The undesired part of the state is removed to another degree of freedom by a controlled transformation, here to another electronic surface. The initial state is purified but its density is reduced. (d) A properly designed decay transfers population back to the initial state and reconstructs its density during a free evolution of the system.

plied to complex quantum systems. The principles of such a control scheme will be demonstrated by a simplified model composed of a single two-level qubit with frequency ω_1:

$$\hat{\mathbf{H}}^0 = \begin{bmatrix} 0 & 0 \\ 0 & \omega_1 \end{bmatrix}, \tag{2}$$

with the two states denoted by $\{|1\rangle_g, |2\rangle_g\}$. The two levels can represent, for example, two spin states or two vibrational levels in a diatomic molecule. The qubit is then influenced by an external noisy field:

$$\hat{\mathbf{H}}_{noise} = \mu f(t) \begin{bmatrix} 0 & 1 \\ 1 & 0 \end{bmatrix} \tag{3}$$

where μ is the dipole moment and $f(t)$ is a white noise function which obeys

$$\langle f(t) \rangle = 0, \quad \langle f(t) f(t') \rangle = \zeta \delta(t - t'). \tag{4}$$

The target of the control is to conserve an initial qubit state protecting it from the noise. We first will describe the route to build a QG for a particular target bit. This approach will then be extended to a general target bit.

A. The conservation of a bit in its ground state

The state of the system is described by a density operator in the energy representation. The target and initial states are chosen as

$$\hat{\rho}^0 = |1\rangle\langle 1| = \begin{pmatrix} 1 & 0 \\ 0 & 0 \end{pmatrix}. \tag{5}$$

The propagation in time of $\hat{\rho}^0$ under the influence of the noise leads to an undesired population on the excited $|2\rangle$ state. To restore the state, the qubit is coupled to an auxiliary qubit with frequency ω_2, $\{|1\rangle_e, |2\rangle_e\}$. The second qubit can be realized, for example, as two vibrational levels within the excited electronic state. The distillation step is achieved by applying the unitary swap transformation

$$\hat{\mathbf{O}}_d = \begin{pmatrix} 1 & 0 & 0 & 0 \\ 0 & 0 & 1 & 0 \\ 0 & 1 & 0 & 0 \\ 0 & 0 & 0 & 1 \end{pmatrix}. \tag{6}$$

The outcome of this transformation is that all the undesired population is transferred to the state $|1\rangle_e$ of the auxiliary e bit. This step cancels also the phase between the two states. The level scheme for the model and the coupling between them is presented in Fig. 2(a).

Note that the transformation is done under Liouville evolution which allows also non-unitary transformations to take place. A possible one-step solution for the QG might be to leave the population in the desired state untouched while moving all the other population to the desired state, e.g., with the distilling operator

$$\hat{\mathbf{O}} \propto \begin{pmatrix} 1 & 0 \\ 1 & 0 \end{pmatrix}. \tag{7}$$

This solution uses the uncontrolled, nonunitary components of the Liouvillian operators. In the limit when the unitary transformations are fast relative to the dumping rate this idea becomes unpractical. We are therefore forced to use a transformation that is close to unitary, and add another step for the completion of the task.

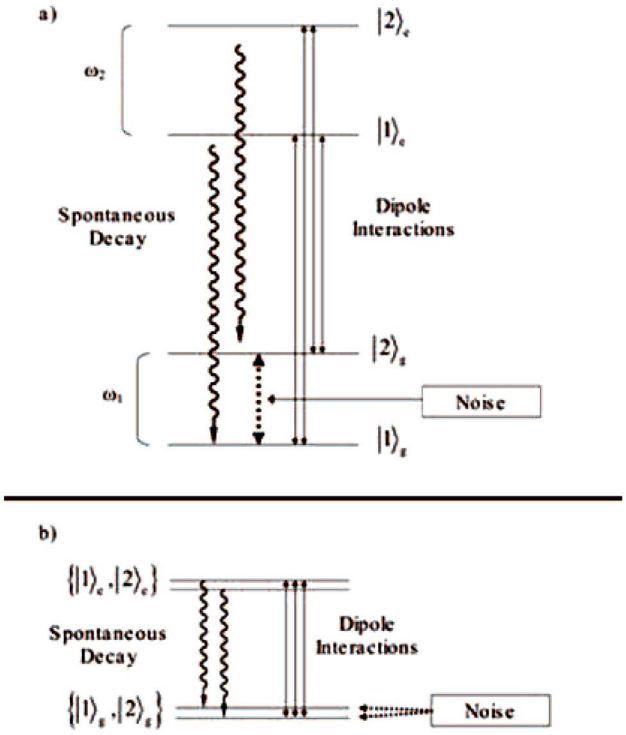

FIG. 2. (Color online) Level scheme for a QG. (a) A QG that conserves a bit on its ground state. A two-level system with frequency ω_1 is influenced by noise. An external field can be applied on the bit to couple it with another bit with frequency ω_2. Spontaneous decay is allowed only as depicted on the figure. (b) A QG that conserves a general bit. The lower (target) bit is composed of two degenerate levels, and so is the upper (control) bit. The external field is coupled between the two bits, while spontaneous decay is allowed only as depicted.

The free-evolution step is generated by the following Liouville-von Neumann equation:

$$\frac{\partial \hat{\rho}}{\partial t} = -\frac{i}{\hbar}[\hat{\mathbf{H}}^0 + \hat{\mathbf{H}}_{noise}, \hat{\rho}] + \mathcal{L}_D(\hat{\rho}) \tag{8}$$

where $\mathcal{L}_D$ is a particular dissipative Liouville superoperator.

$\mathcal{L}_D$ induces a selective decay between the vibrational states: $|1\rangle_e \rightarrow |1\rangle_g$ and $|2\rangle_e \rightarrow |2\rangle_g$. The structure of the decay scheme is chosen to fit intuitively to the goal of avoiding any further mixing due to the decay.[1] Nevertheless, as we will show in Sec. IV, the correction scheme is able to correct also for some imperfect selection rules of quenching; for example a decay induced by the transition-state dipole between vibronic (vibrational+electronic) states, which has the above selection rules.

[1]Simple physical examples for such a scheme might be found in two vertically shifted oscillators coupled by radiation, which can also modify the potential. During the interaction period all the states within the two potentials are coupled by the light. Spontaneous emission, however, will take place at the dark period, and hence only identical levels could be connected due to Frank-Condon overlap terms.

After the distillation step, both the lower and upper bits reside on the target state within the single-bit subspace, i.e., with the correct relative population and phase. The decay step then restores the population from the upper bit, reconstructing the density of the target bit. A cyclic application of this scheme on a quantum system purifies it, reducing the influence of the noise to minimum.

This process can also be considered as a perpetual preparation of the desired state. Note, however, that this desired state itself is never achieved directly in any of the steps. The governor acts by enforcing the conservation of the state by properly aligning the state on the directions of the target.

B. The conservation of a bit in a general state

We next study the preservation of a superposition state which has the form

$$|+\rangle = a|1\rangle_g + b|2\rangle_g \tag{9}$$

with $|a|^2+|b|^2=1$. The general bit description can be obtained from the simple case of Eq. (5) by a unitary rotation.

The governor utilizes the unitary transformation

$$\hat{\mathbf{U}} = \begin{pmatrix} a & b^* & 0 & 0 \\ b & -a^* & 0 & 0 \\ 0 & 0 & a & b^* \\ 0 & 0 & b & -a^* \end{pmatrix}. \tag{10}$$

This unitary operator transforms the basis set from the original basis $\{|1\rangle_g, |2\rangle_g, |1\rangle_e, |2\rangle_e\}$ to a new basis set $\{|+\rangle_g, |-\rangle_g, |+\rangle_e, |-\rangle_e\}$. Now, after the noise influences the initial bit, the original bit can be distilled by the transformed form of the swap operator $\hat{\mathbf{O}}_d$ [cf. Eq. (6)]

$$\hat{\mathbf{O}}_d^g = \hat{\mathbf{U}}\hat{\mathbf{O}}_d\hat{\mathbf{U}}^\dagger = \begin{pmatrix} |a|^2 & ab & a^*b & b^2 \\ a^*b^* & |b|^2 & -a^{*2} & -a^*b \\ ab^* & -a^2 & |b|^2 & -ab \\ b^{*2} & -ab^* & -a^*b^* & |a|^2 \end{pmatrix}, \tag{11}$$

so that under the operator $\hat{\mathbf{O}}_d^g$

$$\hat{\mathbf{O}}_d^g|+\rangle_g = |+\rangle_g, \quad \hat{\mathbf{O}}_d^g|-\rangle_g = |+\rangle_e,$$

$$\hat{\mathbf{O}}_d^g|+\rangle_e = |-\rangle_g, \quad \hat{\mathbf{O}}_d^g|-\rangle_e = |-\rangle_e. \tag{12}$$

It has been noticed [14,15] that nondegenerate qubits are very difficult to handle due to the relative coherent phase that develops under the free evolution. To avoid this problem we take the two bits for the conservation of a general bit as two couples of degenerate states. Initially all of the population is on the target bit. After the distilling transformation both the target and the auxiliary bits are, within the single-bit subspace, on the desired state, i.e., $|+\rangle_{g/e}$, with the right phase between the two states of each of the bits.

The transformation of Eq. (11) corrects the error in both population and phase. The principle of the correction is to move a relative error between two states *within* a single bit to a relative error between two bits. A decay step must then

return back the population from the control bit to the target bit and annihilate the relative errors between the bits. This task is achieved using the same assumption used previously with the allowed transitions $|1\rangle_e \rightarrow |1\rangle_g$ and $|2\rangle_e \rightarrow |2\rangle_g$, while other possibilities are forbidden. The scheme for the general bit conservation is illustrated in the lower panel of Fig. 2.

III. OPTIMAL-CONTROL THEORY FOR NONUNITARY TRANSFORMATION UNDER NON-HAMILTONIAN DYNAMICS

The quantum governor is achieved by the unitary transformations responsible for the distillation. The next step is to find the external field that induces such a transformation. This task is achieved by an inversion process which starts from the unitary operator responsible for the distilling and determines the field. The present description is a modification of the treatment of Ref. [16]. A target transformation for an N-level space is described by the $N \times N$ matrix representing the operator $\hat{\mathbf{O}}$. $\hat{\mathbf{O}}$ is neither necessarily unitary nor orthogonal. Nevertheless, practically it cannot deviate too much from unitarity. Our target is to find the field that generates the transformation $\hat{\mathbf{O}}$ at time $t=T_{trans}$, independent of the initial state.

The density operator is now decomposed into a sum of a complete basis set of operators in the Hilbert-Schmidt space. The complete set of an N-level system density operators contains 2^N Hermitian matrices of dimension $N \times N$. A scalar product between two operators $\hat{\mathbf{A}}$ and $\hat{\mathbf{B}}$ in Hilbert-Schmidt space is defined as [4]

$$(\hat{\mathbf{A}} \cdot \hat{\mathbf{B}}) = \mathrm{Tr}\{\hat{\mathbf{A}}^\dagger \hat{\mathbf{B}}\}. \tag{13}$$

The norm of an operator is therefore $|\hat{\mathbf{A}}| = \mathrm{Tr}\{\hat{\mathbf{A}}^\dagger \hat{\mathbf{A}}\}$. For density operators $|\hat{\rho}| = \mathrm{Tr}\{\hat{\rho}^2\}$ is defined as the purity, $\frac{1}{N} \leqslant |\hat{\rho}| \leqslant 1$, so that $|\hat{\rho}| = 1$ for a pure state and $|\hat{\rho}| = 1/N$ for the maximally mixed state. Note that under unitary dynamics the purity and the entropy of a density operator are conserved. This, however, is not true under dissipative conditions.

For the transformation to be independent of the initial density operator it should change the complete set of base operators $\{\hat{\mathbf{G}}_j^0\}$ to a transformed set. Therefore the desired operation $\hat{\mathbf{O}}$, maps each of the basis set operators to a new target operator

$$\hat{\mathbf{G}}_j^{target} = \hat{\mathbf{O}} \hat{\mathbf{G}}_j^0 \hat{\mathbf{O}}^\dagger. \tag{14}$$

Under unitary transformation the complete orthonormal set is transformed to another complete orthonormal set. For nonunitary transformations this statement is not true. The chosen functional for the inversion procedure should reflect deviations between the propagated operators and the target set of operators. Since the target set of operators $\{\hat{\mathbf{G}}_j^{target}\}$ does not conserve the initial norm, the optimal-control functional is defined at the initial time as

$$\tilde{F} = \sum_j (\hat{\mathbf{G}}_j^0 \cdot \hat{\mathbf{G}}_j^{result}) \tag{15}$$

where the set $\{\hat{\mathbf{G}}_j^{result}\}$ is obtained by propagating the set of target operators $\{\hat{\mathbf{G}}_j^{target}\}$ *backward* in time. Once the target is achieved $F = 2^N$.

Two additional constraints are imposed: (1) The reverse time evolution of the system is also governed by the Liouville–von Neumann equation; and (2) the total field energy has to be minimized. To meet these demands a modified functional is employed:

$$F = \tilde{F} - \sum_j \int_{T_{trans}}^0 \left[\left(\frac{\partial \hat{\mathbf{G}}_j}{\partial t} - \mathcal{L}^*(\hat{\mathbf{G}}_j) \right) \cdot \hat{\mathbf{B}}_j \right] dt - \int_{T_{trans}}^0 \lambda(t) |\varepsilon|^2 dt. \tag{16}$$

$\hat{\mathbf{B}}_j$ are 2^N operator Lagrange multipliers, and $\lambda(t)$ is a time-dependent scalar Lagrange multiplier. An extremum for F is obtained by a variation of F with respect to $\delta \hat{\mathbf{G}}_j$ and the field. Following Ref. [16], the equations of motion for the reverse propagation of the G_j's become

$$\frac{\partial \hat{\mathbf{G}}_j}{\partial t} = + \frac{i}{\hbar} [\hat{\mathbf{H}}, \hat{\mathbf{G}}_j] + \mathcal{L}_D(\hat{\mathbf{G}}_j) \tag{17}$$

with the initial conditions $\hat{\mathbf{G}}_j(T_{trans}) = \hat{\mathbf{G}}_j^{target}$, and for the forward time propagation of the $\hat{\mathbf{B}}_j$ operators

$$\frac{\partial \hat{\mathbf{B}}_j}{\partial t} = - \frac{i}{\hbar} [\hat{\mathbf{H}}, \hat{\mathbf{B}}_j] + \mathcal{L}_D(\hat{\mathbf{B}}_j) \tag{18}$$

and $B_j(0) = G_j^0$. It should be noticed that in both forward and backward propagation the dissipative part generated by $\mathcal{L}_D$ causes relaxation.

Applying Krotov's iterative method to obtain monotonic increase toward the objective at each iteration leads to the field at each new iteration at the time t:

$$\epsilon^{new}(t) = \epsilon^{pre}(t) + \lambda C(t) \sum_j \{[\hat{\mu}, \hat{\mathbf{G}}_j(t)] \cdot \hat{\mathbf{B}}_j(t)\} \tag{19}$$

where $C(t)$ is a time-dependent envelope function. λ is a strategy parameter. Large values of λ will cause rapid changes of the field at each iteration.

The size of the computation effort to find the field is believed to grow exponentially with the number of bits for systems that evolve under unitary dynamics [12]. For the present case of nonunitary dynamics it is expected to be even worse. This expected result originates from the fact that under nonunitary dynamics decoherence destroys interfering pathways with long periods.

IV. SIMULATION AND RESULTS

A. Protecting a bit in its ground state

The application of the QG in protecting a target bit of the form of Eq. (5) is now demonstrated. The first step of the procedure is to calculate the field required for the generation of the distilling transformation $\hat{\mathbf{O}}_d$ [cf. Eq. (6)]. Two main time scales dominate the QG model: (1) τ_{trans}, the time du-

TABLE I. Parameters used in the simulation: Δ is the electronic energy gap, ω_j is the vibrational frequency for the jth electronic state, τ_{trans} is the duration of the distillation transformation, Γ is the decay rate, and τ_{free} is the period of a correction cycle.

Parameter	Value
Δ	0.06601 hartree
$\hbar\omega_1$	$7.2449716268\times10^{-4}$ hartree
$\hbar\omega_2$	$5.3746313155\times10^{-4}$ hartree
τ_{trans}	1.08 ps
Γ^{-1}	10.0 ps
τ_{free}	241 ps

ration for the field-derived transformation, and (2) τ_{free}, the period of free propagation, where $\tau_{trans}\ll\tau_{free}$. The characterizing parameters of the four levels of the model are taken as the two couples of the two lowest vibrational states within the first two electronic states of the Na_2 molecule. Table I summarizes the parameters used in the simulations.

The operations are carried out in a four-level space. Due to the decay of the upper bit, it can be assumed that when the controlled transformation is applied, all the population is at the lower bit. Hence, only a basis set for a single bit, i.e., the lower bit, operation subspace within a four-level system is needed. The time evolution generated by the Liouville–Von Neumann equation was calculated by the Newton polynomial expansion method [17].

Figure 3 displays the infidelity of the transformation, $\log_{10}(1-F/2^n)$, vs the number of iterations. n is the number of basis states involve in the operation, here 2. The two inset panels of Fig. 3 show the resulting fields and their Fourier transforms which generate an infidelity close to -12. The two peaks in the frequency domain are the result of the initial guess which initiated the optimization process, $\epsilon(t)\propto\cos(\Delta t)$, where Δ is the vertical energy gap between the two electronic states.

At the second step, the target bit $\rho^0=|1\rangle_g\langle 1|_g$ is propagated freely for a duration τ_{free} with the additional distilling trans-

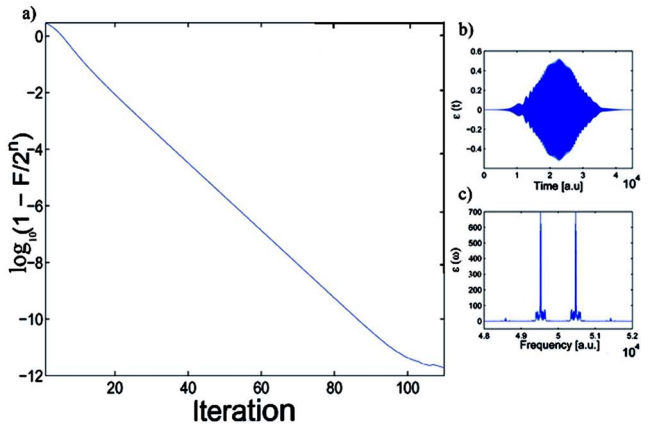

FIG. 3. (Color online) (a) Infidelity of the transformation gate $\hat{\mathbf{O}}_d$ versus the number of iterations, and (b) and (c) the time and frequency dependency of the field.

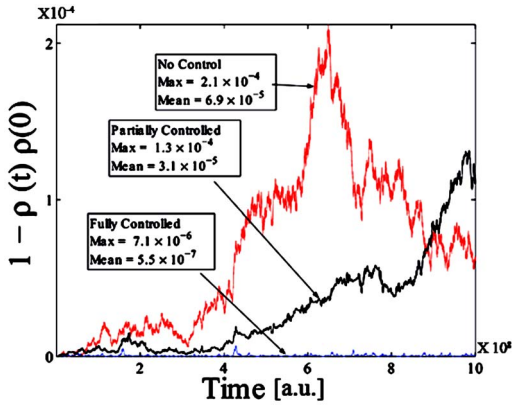

FIG. 4. (Color online) The deviation of the bit vs time for the uncontrolled (red), partially controlled (black), and fully controlled (blue) cases. The deviation is defined as $1-[\hat{\rho}^0\cdot\hat{\rho}(t)]$. See the text for the parameters used for the simulation.

formation. The white noise function for the propagation [cf. Eq. (3)] is modeled as

$$f(t)=Ns(t) \tag{20}$$

where N is the noise intensity and $-0.5<s(t)<0.5$ is generated from a uniform random distribution. The decay rates are taken to be $\Gamma_{11}^{-1}=\Gamma_{22}^{-1}$. For comparison, three calculations were performed with the same noise parameters.

(1) A reference propagation: the system is propagated with noise without any correction. The red line in Fig. 4 represents the value of $R=1-[\hat{\rho}^0\cdot\hat{\rho}(t)]$ versus time. A significant deviations from the initial bit develops, up to $R=0.02\%$, due to the noise. The time-averaged deviation is about one-third of the maximal deviation.

(2) A partially controlled propagation: the distilling transformation is applied on the bit at each τ_{free}, but no decay between the bits was allowed. The black line in Fig. 4 displays the deviations of the density matrix from the target $\hat{\rho}^0$ vs time, for this case. According to the transformation $\hat{\mathbf{O}}_d$ any remains of population on the upper bit will be transferred back to the lower bit and ruin the efficiency of the noise reduction. As expected, the growth of deviations from the target bit develops here almost at the same rate as in the previous case. The maximal deviation is 0.01% and the average is again one-third of the maximal value.

(3) Fully controlled propagation: the system is propagated with both the distilling transformation and the decay period between the bits. The blue line in Fig. 4 represents deviations of the density matrix from the target for the fully controlled propagation. It can clearly be seen that the full scheme works well. The maximal deviation under the fully controlled propagation is reduced to $(7\times10^{-4})\%$ and the average to approximately $(6\times10^{-5})\%$. Figure 5 is a blowup of this line. The influence of the very frequent corrections is clearly visible. The system is more stable by two orders of magnitude on average under the QG scheme.

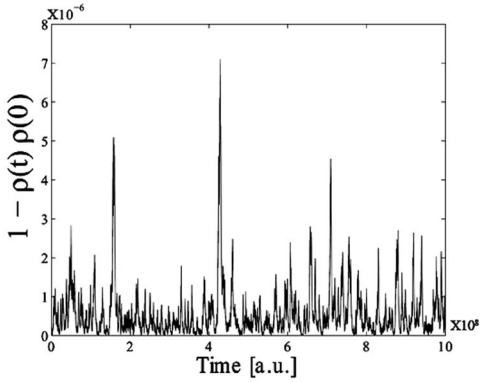

FIG. 5. A blowup of the deviation of the bit vs time for the fully controlled system: A distilling transformation is apply every τ_{free} =241 ps.

Changes of some of the parameters of the system, e.g., taking τ_{free} to be smaller, can stabilize the system even further.[2]

B. Conservation of a general bit and an investigation of the necessary features for a QG

For a general bit case the normalized state was chosen as the target bit,

$$|+\rangle_g = |+\rangle = \frac{1}{\sqrt{1+b_n^2}}(|0\rangle - ib_n|1\rangle), \tag{21}$$

and b_n randomly chosen to be equal to 0.231 138 513 574 29. The two bits were chosen as two pairs of degenerate two-level systems. The optimal field for this transformation gate was converged to the same accuracy as in the previous section with approximately the same speed of convergence

The noise model influenced directly both the population and the phase between the states:

$$\hat{\mathbf{H}}_{noise} = \mu f(t)\begin{bmatrix} -1 & 1 \\ 1 & 1 \end{bmatrix}. \tag{22}$$

To gain more insight into the necessary features needed for a QG to work properly several simulations for mutated QGs are presented. Two conventions for the characterizing parameters are employed. The first one is identical to the previous one:

$$R = 1 - [\hat{\rho}^0 \cdot \hat{\rho}(t)]. \tag{23}$$

A scheme which conserves low values of R can be defined as a fully conserved scheme. The distilling transformation aligns the bit in the right direction, i.e., with the correct relative phase and population between the two states. A bit can deviate from the target bit in its norm but still conserves a high resemblance to it with respect to the correct phase and population. A normalized deviation is defined as

$$R_n = 1 - \frac{[\hat{\rho}^0 \cdot \hat{\rho}(t)]}{|\hat{\rho}(t)|} = 1 - \frac{[\hat{\rho}^0 \cdot \hat{\rho}(t)]}{\sqrt{(\hat{\rho}(t) \cdot \hat{\rho}(t))}}. \tag{24}$$

The upper and lower panels of Fig. 6 represent the measures R and R_n for five simulations with the same noise parameters. The results are concentrated in Table II.

Five test cases are simulated.

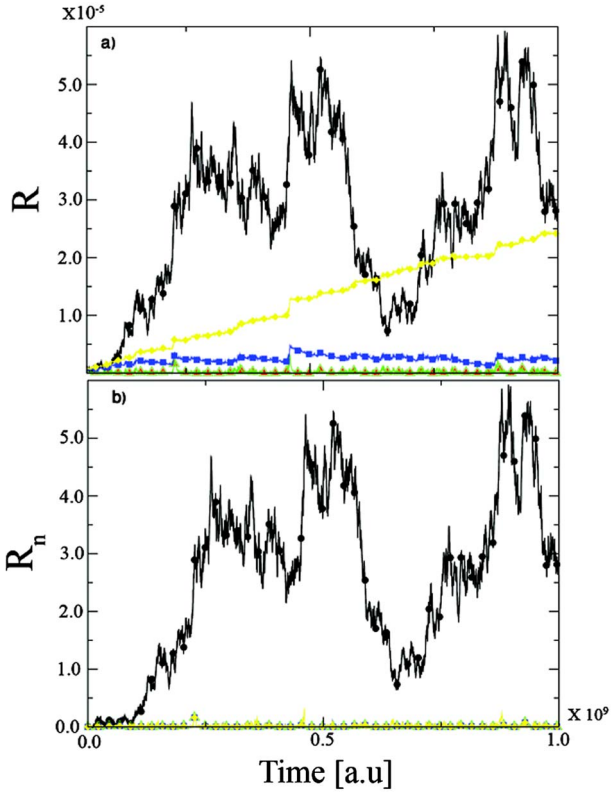

FIG. 6. (Color online) The deviation of a general bit vs time for the cases of uncontrolled propagation [(black) circles], and equal [(red) closed triangles], different [(green) open triangles], and exchanged [(blue) squares] decay rates, and for the case where the decay channel is not directed back to the subspace of the controlled bit [(yellow) diamonds]. The two panels display (a) R, the unnormalized, and (b) R_n the normalized deviations, respectively. See the text for a more detailed description of the various cases.

TABLE II. Deviations from a general target bit for five different test cases (see the text for details). The columns display the maximal and the average of the deviations R and R_n for the five cases.

	R^{max}	R_n^{max}	$\langle R \rangle$	$\langle R_n \rangle$
1	5.9×10^{-5}	5.9×10^{-5}	2.9×10^{-5}	5.9×10^{-5}
2	3.1×10^{-6}	3.1×10^{-6}	2.0×10^{-7}	1.3×10^{-7}
3	3.1×10^{-6}	3.1×10^{-6}	2.0×10^{-7}	1.3×10^{-7}
4	4.8×10^{-6}	3.1×10^{-6}	2.2×10^{-6}	1.3×10^{-7}
5	2.4×10^{-5}	3.1×10^{-6}	1.2×10^{-5}	1.3×10^{-7}

[2]Several numerical tests were performed for the present case as well as for the case of unitary transformation under unitary time evolution of Ref. [12]. Typically the difficulty in achieving the optimal field depended very weakly on the nature of the desired gate.

(1) A reference propagation without any correction depicted by the black line with closed circles, $R=R_n$.

(2) A fully controlled scheme with equal decay rates $\Gamma_{11}^{-1}=\Gamma_{22}^{-1}=10$ ps, depicted by the (red) line with the closed triangles. The efficiency of the QG is the same as for previous case of the ground-state bit. Both R and R_n are conserved to values well below the uncorrected propagation. The system is more stable by a factor of 20 at the worst case and by more than a factor of 200 on average.

(3) This scheme is identical to (2), but with different decay rates $\Gamma_{11}^{-1}=\frac{1}{10\pi}\Gamma_{22}^{-1}=10$ ps. Only selective decay is allowed. The results are depicted by the (green) line with open triangles. The scheme seems to work at the same efficiency as the previous case. The relative phase that develops *between* the two bits during the propagation due to their different energies is destroyed by the decay so that only the inner phase between the states is conserved.

(4) In this case the decay channels were switched so that the decay channels are $|1\rangle_e \rightarrow |2\rangle_g$ and $|2\rangle_e \rightarrow |1\rangle_g$. The results [(blue) line with closed squares] show that under this scheme the noise is accumulated and the unnormalized deviation from the target is constantly growing. However, the accumulated error is still bearable, so that the mutated QG manages to transform the undesired part to the other bit and R_n is still conserved.

(5) In this test case [(yellow) line with closed diamonds], it was assumed that the population of the upper bit decays by some drain channel to a bath outside of the system. Under this scheme the remaining bit is well conserved but the norm of the state is reduced significantly.

Another four test-case simulations are presented in Fig. 7. The numerical results are summarized in Table III. The lines with (black) circles and (red) triangles present, as on the previous demonstration, the uncontrolled and fully controlled QGs. The case presented by the line with the (blue) squares has a nondegenerate upper bit. The nondegenerate states of the bit develop a phase that destroys completely the correction scheme. It is interesting to note that just as in the previous example, a difference between the two decay rates does not cause a significant change in the efficiency of the QG.

The last case that was checked [the line with (yellow) diamonds] is a scrambling of the upper bit transformation, which makes a Hadamard transformation to the upper bit consecutive to the regular distilling transformation. The result of this mutation is a bearable accumulated error, which is moved constantly to the upper bit and leaves the lower bit close to the target state, but with lower norm.

V. DISCUSSION AND CONCLUSIONS

An integral and crucial part of quantum computing and information research is devoted to quantum error correction (QEC) [18–20]. The main question in QEC is the following. Suppose A is sending quantum information to a receiver B. An unavoidable influence of a noise may distort the quantum information with probability $p<1/2$. How would B be able to reconstruct the data that were sent to A? The solution to this problem is usually given by redundancy. Before sending his quantum information, A must duplicate his data in several copies from which B would be able to withdraw the original data to a very high accuracy.

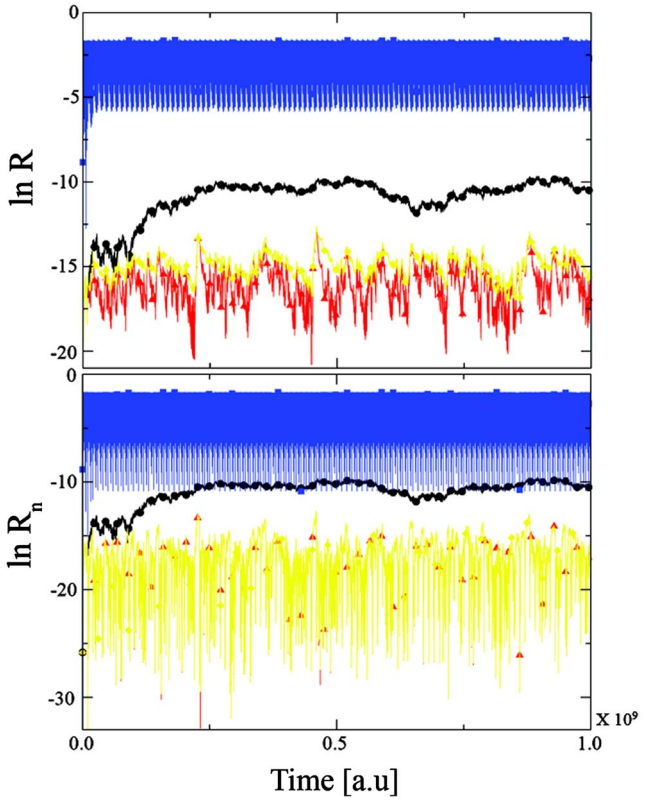

FIG. 7. (Color online) Logarithm of the deviation of a general bit vs time for the cases of uncontrolled propagation [(black) circles], equal decay rates [(red) triangles], nondegenerate bit [(green) squares], and scrambled transformation [(yellow) diamonds]. The two panels display (a) R, the unnormalized, and (b) R_n, the normalized deviation. See the text for a more detailed description of the various cases.

The task of building a quantum governor is close to QEC, but is different in both motivation and strategy. A QG main goal is to reduce the influence of noise on the channel between A and B, that is, to reduce p. Moreover, the strategy to achieve the control uses mainly the system itself and does not create extra information. Considering the fact that the scaling of the difficulty of building quantum computers is believed to be exponential in the size of the system, it seems that the task of protecting a single bit from decoherence might be more important for quantum computing than the ability to use QEC.

TABLE III. Deviations from a general target bit for four different test cases (see the text for details). The columns display the maximal and the average of the deviations R and R_n for the four cases.

	R^{max}	R_n^{max}	$\langle R\rangle$	$\langle R_n\rangle$
1	5.8×10^{-5}	5.8×10^{-5}	2.5×10^{-5}	2.5×10^{-5}
2	3.1×10^{-6}	3.1×10^{-6}	1.9×10^{-7}	1.3×10^{-7}
3	2.1×10^{-1}	1.9×10^{-1}	1.0×10^{-1}	9.4×10^{-2}
4	3.1×10^{-6}	3.1×10^{-6}	4.1×10^{-7}	1.3×10^{-7}

The target entitled here as the quantum governor can be stated in two versions.

(1) The frail QG—one or more of the system expectation values is constrained, e.g., energy, angular momentum, etc. This constraint is quite similar to the original constraint imposed by Watt on his classical governor. The similarities between such a QG and error corrections are seemingly minor.

(2) The robust QG—the task of interest is the full conservation of the state of the system, and not only one of its observables. This demand is more difficult than the one imposed by the Watt governor but it brings the robust QG closer to the error correction field.

Due to the fact that uncommutative operators cannot be measured simultaneously, it is well understood that feedback control might be applicable to several kinds of frail QG, but surely not for any robust QG.

In this paper the QG problem was solved for the robust case for a model two-level system. In this case the difference between the two versions is not large. The robust QG problem is also related to the problems of refocusing and (dynamical) decoupling [21–24]. Both approaches aim to reduce influences of noise coupled to a quantum system. However, the strategies of the two schemes are totally different. The QG problem is a *state*-oriented problem. It demands the conservation of known states from the influence of noise of an unknown form. A treatment of the noise in terms of stochastic quantum equations (see, for example, [25–27]) is therefore unnecessary. The problems of refocusing and decoupling are *noise*-oriented problems. They try to immunize unknown states against a noise with a known form. Accordingly, the solutions to the last couple of problems, e.g., the bang-bang method and its derivatives, use the known structure of the noise in order to build the appropriate immune decoupling.

To summarize, in this paper the fundamental demands for the task of building a quantum governor were developed. The basis was set for a scheme to achieve automatic control on simple quantum systems. The scheme was demonstrated through simulations on a two-level system. A reduction of the noise by more then two orders of magnitude was achieved. The necessary features of a working QG under the present scheme were examined.

The extension of the present scheme to more complicated systems requires additional study. Several other schemes and methods to achieve QG, for example the use of the quantum Zeno paradox, could be purposed. The exploration of these possibilities is still under way.

ACKNOWLEDGMENTS

This work was supported by the Israel Science Foundation. The authors would like to thank Jose P. Palao for his assistance, and Daniel Lidar for fruitful discussions.

[1] A. Steane, Rep. Prog. Phys. **61**, 117 (1998).
[2] D. P. DiVincenzo, Science **270**, 255 (1995).
[3] S. Lloyd, Science **261**, 1569 (1993).
[4] M. A. Nielsen and I. L. Chuang, *Quantum Computation and Quantum Information* (Cambridge University Press, Cambridge, U.K., 2000).
[5] K. Zhou, J. Doyle, and K. Glover, *Robust and Optimal Control* (Prentice-Hall, Englewood Cliffs, NJ, 1996).
[6] W. L. Brogan, *Modern Control Theory* (Prentice-Hall, Englewood Cliffs, NJ, 1991).
[7] A. C. Doherty, S. Habib, K. Jacobs, H. Mabuchi, and S. M. Tan, Phys. Rev. A **62**, 012105 (2000).
[8] S. Habib, K. Jacobs, and H. Mabuchi, Los Alamos Sci. **27**, 116 (2002).
[9] A. J. Berglund and H. Mabuchi, Appl. Phys. B: Lasers Opt. **B78**, 653 (2004).
[10] D. A. Steck, K. Jacobs, H. Mabuchi, T. Bhattacharya, and S. Habib, Phys. Rev. Lett. **92**, 223004 (2004).
[11] J. P. Palao and R. Kosloff, Phys. Rev. Lett. **89**, 188301 (2002).
[12] J. P. Palao and R. Kosloff, Phys. Rev. A **68**, 062308 (2003).
[13] S. E. Sklarz and D. J. Tannor, Phys. Rev. A **61**, 053404 (2004).
[14] D. Bacon, K. R. Brown, and K. B. Whaley, Phys. Rev. Lett. **87**, 247902 (2001).
[15] M. I. Dyakonov, Opt. Spectrosc. **95**, 261 (2003).
[16] A. Bartana, R. Kosloff, and D. J. Tannor, J. Chem. Phys. **106**, 1435 (1997).
[17] W. Huisinga, L. Pesce, R. Kosloff, and P. Saalfrank, J. Chem. Phys. **110**, 5538 (1999).
[18] A. M. Steane, Proc. R. Soc. London, Ser. A **452**, 2551 (1996).
[19] P. W. Shor, Phys. Rev. A **52**, R2493 (1995).
[20] A. M. Steane, Philos. Trans. R. Soc. London, Ser. A **356**, 1739 (1998).
[21] M. Ban, J. Mod. Opt. **45**, 2315 (1998).
[22] L. Viola, E. Knill, and S. Lloyd, Phys. Rev. Lett. **82**, 2417 (1999).
[23] L. Viola and S. Lloyd, Phys. Rev. A **58**, 2733 (1998).
[24] K. Khodjasteh and D. A. Lidar, Phys. Rev. Lett. **89**, 197904 (2002).
[25] H. M. Wiseman and G. J. Milburn, Phys. Rev. Lett. **70**, 548 (1993).
[26] S. Mancini, D. Vitali, and P. Tombesi, Phys. Rev. Lett. **80**, 688 (1998).
[27] D. Vitali, S. Mancini, L. Ribichini, and P. Tombesi, Phys. Rev. A **65**, 063803 (2002).